

## Positive Plate for Carbon Lead-Acid Battery

Andrzej Czerwiński<sup>1,2,\*</sup>, Zbigniew Rogulski<sup>1</sup>, Szymon Obrębowski<sup>1</sup>, Jakub Lach<sup>1</sup>, Kamil Wróbel<sup>1</sup>, Justyna Wróbel<sup>1</sup>

<sup>1</sup> Industrial Chemistry Research Institute, Rydygiera 8, 01-793 Warsaw, Poland

<sup>2</sup> Faculty of Chemistry, Biological and Chemical Research Centre, University of Warsaw, Żwirki i Wigury 101, 02-089 Warsaw, Poland

\*E-mail: [aczerw@chem@uw.edu.pl](mailto:aczerw@chem@uw.edu.pl)

Received: 7 May 2014 / Accepted: 9 June 2014 / Published: 16 June 2014

---

Positive plates for the carbon lead-acid battery (CLAB) with porous carbon grids coated with lead have been prepared and tested. Lead coating thickness in the range between 20 and 140 micrometers has been shown to positively influence the discharging profile and the cyclic lifetime of the plates. Thicker coating improves both the cyclic life and discharge performance. The increase of battery specific energy by 50% is expected by employing the lightweight carbon grid with 60  $\mu\text{m}$  lead coating for positive plates, and 20  $\mu\text{m}$  for negative.

---

**Keywords:** lead-acid battery, positive plate, reticulated vitreous carbon, energy storage

### 1. INTRODUCTION

Since the beginning of the 20<sup>th</sup> century, the lead-acid battery has been the most widely used power source for a number of applications, namely, combustion engine starting, small traction, load leveling. However, the main disadvantage still remains, which is its low energy density and specific capacity when compared with other battery systems. The main reason for this is the high contribution of plates' grids made of lead alloys to the total mass of the battery (up to 25 %). As an alternative for lead, reticulated vitreous carbon (RVC) has been proposed by Czerwiński as a grid material [1]. This lightweight, conducting, porous carbon material has an apparent density as low as 0.048 g cm<sup>-3</sup>. Its continuous conductive structure and good chemical resistivity to concentrated aqueous and non-aqueous media makes it a great choice for R&D not only for the lead-acid but also for other battery systems and supercapacitors [8-14].

Today, it is known that porous carbon can be used for the production of the lead-acid-battery negative plates. Such batteries employing negative plates based on porous graphite are commercially available from Firefly International Energy Co. [15]. The key features of those new batteries are much faster recharging and better cycle life compared with the traditional ones. In our recent papers we demonstrated that the bare RVC as well as the RVC covered with Pb can be successfully employed as grid material for the negative plate and such an electrode can be readily electrochemically characterized. The performance of the negative plate with the new type of carrier/collector proved to be very good [16-19].

Bare RVC, as well as other types of carbon materials, is not suitable as a grid material for the positive plates of the lead-acid batteries. This problem was investigated by several scientific groups. Jang et. al. evaluated the electrochemical behavior of graphitized and non-graphitized carbon foams in sulfuric acid environment in the potential range in which the lead-acid battery operates [20]. It was confirmed that a graphite substrate undergoes deep oxidation in sulphuric acid media at potential values higher than 1 V vs. SSE (mercury/mercurous sulfate electrode), i.e., values experienced by the positive plate. Although non-graphitized carbon was found relatively stable under the above high-potential conditions, a rise of the oxidation current above 1,1 V was evident in the voltammetric curves. This behavior was not explained, however, it can be implied that the oxygen evolution reaction takes place at the carbon surface. Batteries with graphitized carbon foam employed as both positive and negative current collectors in the case of the positive plate showed a steep potential drop and failed within a few minutes of the first discharging. Chen and coworkers synthesized non-graphitized carbon foams by the template method from a petroleum pitch and employed them as a plate grid in a small lead-acid battery [21]. They obtained good results for the negative plates based on bare carbon [22, 23]. The positive plates suffered from a very low charge acceptance, which has been ascribed to the parasitic reaction of oxygen evolution on carbon during the charging step [21]. Basic cyclic voltammograms (CVs) for the bare carbon foam cycled in the positive plate potential regime resembled those of Jang et al. Glassy carbon (GC), whose electrochemical behavior should be most similar to the RVC's, was examined in sulfuric acid solutions by Dekanski et al. [24]. They observed that the GC electrode surface deteriorated heavily after anodizing in sulfuric acid at potentials  $> 2$  V vs. SCE (standard calomel electrode).

The layer between the grid of the positive plate in the lead-acid battery and the positive active mass (PAM) is a complex mixture of lead oxides and sulfates formed during plate curing and formation. The layer is also transforming during the cyclic charging/discharging of the plate. This "corrosion" layer and the corrosion layer/PAM interface keeps the grid metal in electrical and mechanical connection with the PAM. Applying a uniform, crack-free lead/lead-alloy coating with a controlled thickness over the whole carbon matrix surface and with a composition tailored for the specific duty type appears to be the only way for obtaining successful porous-carbon-based positive plates. Results patented at the beginning of the 1990's by Czerwiński showed that RVC plated with a thin layer of lead and lead dioxide can exhibit the same electrochemical properties as pure lead [1-6], which suggests the validity of the plating concept. Das and Mondal investigated the electrochemical behavior of lead- and PbO<sub>2</sub>-covered graphite as the lead-acid battery electrodes [25]. They showed that lead-plated graphite can be successfully used for designing a single cell, cyclable lead-acid battery

[26]. Gyenge et al. used RVC plated with a thick Pb-Sn layer (250-300  $\mu\text{m}$ ) as the positive plate grid [27, 28]. Their cell completed over 300 cycles at 25% depth of discharging (DOD). Lately Wen has published a lead-acid battery design employing a pitch-based carbon foam plated with a 50  $\mu\text{m}$ -thick lead layer [29]. Recent Kirchev's results, who used recyclable cardboard soaked with resole as a precursor for honeycomb PbSn-plated carbon matrices seems also to be very promising [30]. Recently we have demonstrated the performance of the 2 V flooded cell constructed from negative and positive plates (lead and lead dioxide) based on reticulated vitreous carbon [31]. Studied cell completed over 65 charge/discharge cycles at 50% depth of discharge without losing its nominal capacity. For higher discharge currents at 100% DOD the cyclic lifetime is limited as a result of grid corrosion which is probably due to relatively thin, non-alloyed pure lead grid coating. However, very promising capacity values for 20-h discharge rate at the level of 120 A h  $\text{kg}^{-1}$  PAM, 170 A h  $\text{kg}^{-1}$  NAM have been obtained

Although pure lead has many disadvantages as a coating, when compared with adequate lead alloys, i.e., faster corrosion at open circuit conditions, lower conductivity, worse mechanical properties (so nowadays it is used only in a few stand-by applications), it can still be successfully employed for fundamental plate research. Besides preparing the positive plates with a new type of grid and examining their quality after the formation process, the major goal of the present work was to study the discharging parameters and the cycle lifetime of the positive plates based on the RVC covered with Pb layers of different thickness.

## 2. EXPERIMENTAL

RVC with 20 p.p.i. (pores per inch) porosity grade, purchased from ERG, Material and Aerospace Corporation, was chosen as the most suitable for this research. The average dimensions of RVC substrates cut were 44 x 75 mm with a thickness ca. 5 mm. The electrical contact between Pb and RVC was casted using melted lead. The RVC electrodes assembled in this way were used as cathodes in lead electroplating. The electroplating was performed in a methane sulfonate bath made and supplied by Aurotech (Warsaw, Poland). The plating efficiency for this type of bath is 100% for current ranges, with which shiny lead deposits are obtained. Thicknesses of the Pb layers were calculated from the deposit weights and the real surface area of the RVC [32]. The calculation of lead deposits thickness is in the agreement with obtained SEM pictures. The electrodes surface morphology was studied with a LEO 435VP scanning electron microscope (SEM).

The RVC/Pb grids were pasted with a standard SLI-type paste obtained from Jenox Ltd (Poland). Pastes taken from the mixers at the Jenox's production line needed to be slightly watered in order to reduce their density and facilitate manual pasting of the relatively thick RVC/Pb grids. The average amount of the paste pressed into each collector was 40 g and 20g, which was predicted to give 5 Ah and 2 Ah of capacity, respectively. Plates were cured in an industrial curing chamber in a two-step process until the amount of moisture in the mass dropped below 0.5%. The BET area of the obtained active mass was 1.50  $\text{m}^2/\text{g}$  and the average crystal size was 4,0  $\mu\text{m}$ . To build a test cell, the positive plate prepared was enclosed in an SLI-type polyethylene ribbed separator and placed between

two negative plates. The amount of the active mass in the negative plates was in excess compared with the amount of active mass in the positive electrode to ensure complete reaction in the latter. Such a two volt assembly has been placed inside a container. In order to measure the potential of the individual positive plates the cell was equipped with a Hg/Hg<sub>2</sub>SO<sub>4</sub>/1M H<sub>2</sub>SO<sub>4</sub> reference electrode (MSE). Figure 1 presents a scheme of the complete cell.

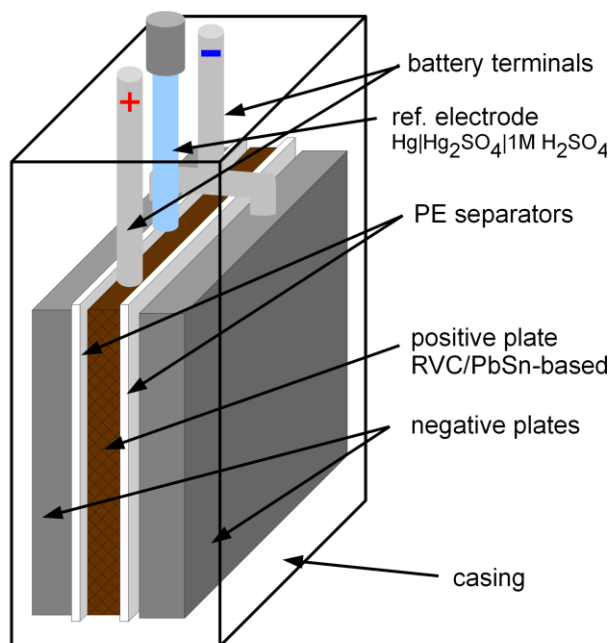


**Figure 1.** Scheme of three-electrode lead-acid cell for positive plate testing.

The assembled cell was filled with an excess of electrolyte for cell formation (21% H<sub>2</sub>SO<sub>4</sub>). During the soaking, which lasted 4 hours, the electrolyte temperature was kept below 40°C. The cell formation was conducted at a constant 0.067C current for 45 hours. After the formation was ended, the electrolyte was exchanged for a standard electrolyte (35% H<sub>2</sub>SO<sub>4</sub>). At the beginning of tests, every cell was subjected to two charge/discharge cycles at 0.05 C discharging current. After that it was cycled consecutively four times using discharging currents from 0.16 C to 0.78 C. Next the cells were cycled consecutively at 0.05 C discharging current. The cutoff voltage during the discharge was 1.75 V for currents below 0.5 C and 1.6 V for currents over 0.5C. After each discharge, the cells were immediately charged using a two-step constant-current/constant-voltage method (charging parameters: 0.08C until 2.4 V is reached and 2.4 V hold for 5 to 7 hours). All electrochemical measurements were made at room temperature using an ATLAS-SOLLICH 961 (Poland) battery tester.

### 3. RESULTS AND DISCUSSION

In preliminary experiments with cells employing positive plates based on bare RVC grids we recorded very low discharging voltages and did not reach reasonable capacities. The cells OCVs were at the level of 2.09-2.12 V, which means that some amount of  $\text{PbO}_2$  was formed during the formation step. However, the formation efficiency was almost zero. Additionally, we noticed a very fast deterioration of the carbon matrix which exhibited a significant loss of mechanical properties after the formation. The mechanical deterioration appeared due to a couple of reasons. First, the carbon was subjected to an oxidizing environment during the curing procedure. Then, long anodizing of the glassy carbon in sulphuric acid solutions lead to its deep corrosion through the process involving surface activation and graphite oxide phase growth. An additional reason for the RVC matrix weakening are possible redox reactions between carbon and lead dioxide.

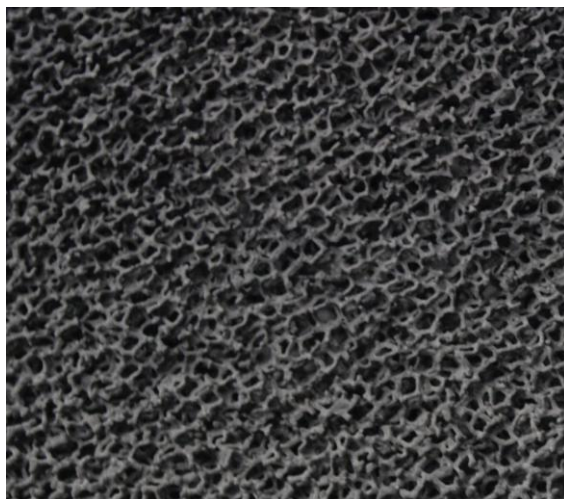


**Figure 2.** Picture of RVC collector covered with lead.



**Figure 3.** Picture of RVC-based lead-acid positive electrode.

To protect the bare RVC surface against unwanted reactions, the matrices have been plated with thin lead layers. Fig. 2a shows a picture of the Pb/RVC carrier for the positive electrode (RVC coated with thin layer of lead) [18,19]. Fig. 2a demonstrates that the carbon surface was evenly covered with a lead layer. A cured positive plate obtained by hand-pasting the RVC/Pb grid is depicted in Fig. 2b. The thickness of the as-prepared positive plate was 5-6 mm.

The quality of the lead coatings on the RVC obtained by electrodeposition was examined using SEM imaging. Fig. 3 presents an RVC collector covered with lead. One can see the coating is uniform over the whole surface of the pictured large section of the sample. Fig. 4 shows a cross section of RVC/Pb filaments coated with a thick layer of lead. Despite its thickness the lead coating varies ca. 15% over the filament cross section, its adhesion is very good and it is impossible to remove the layer mechanically.

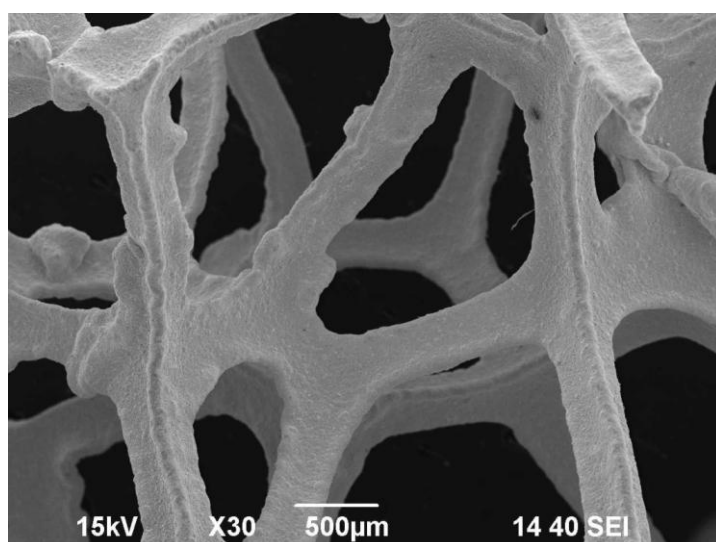


Figure 4. SEM image of RVC collector covered galvanically with lead.

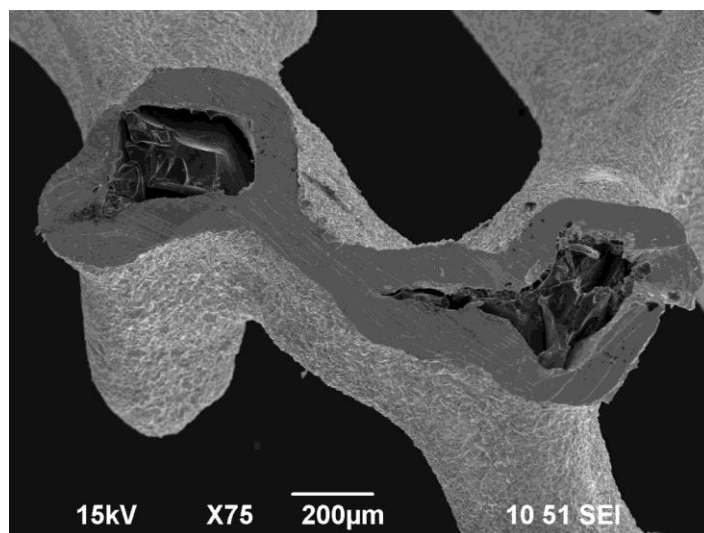
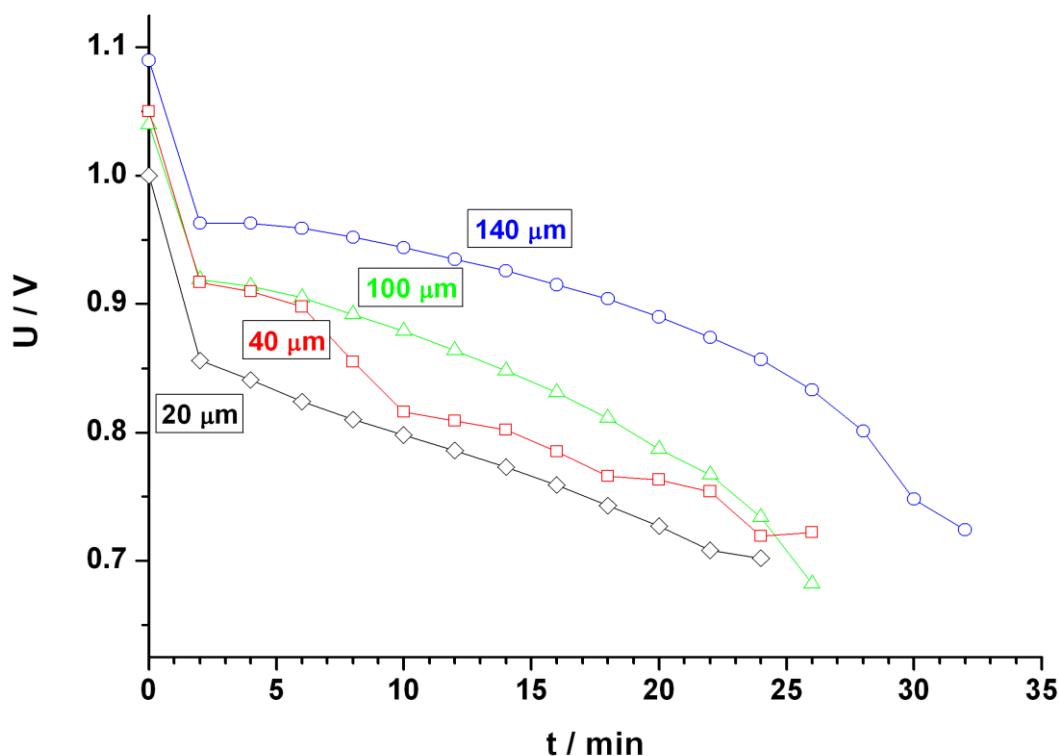


Figure 5. SEM image of cross section of the RVC collector covered galvanically with lead.

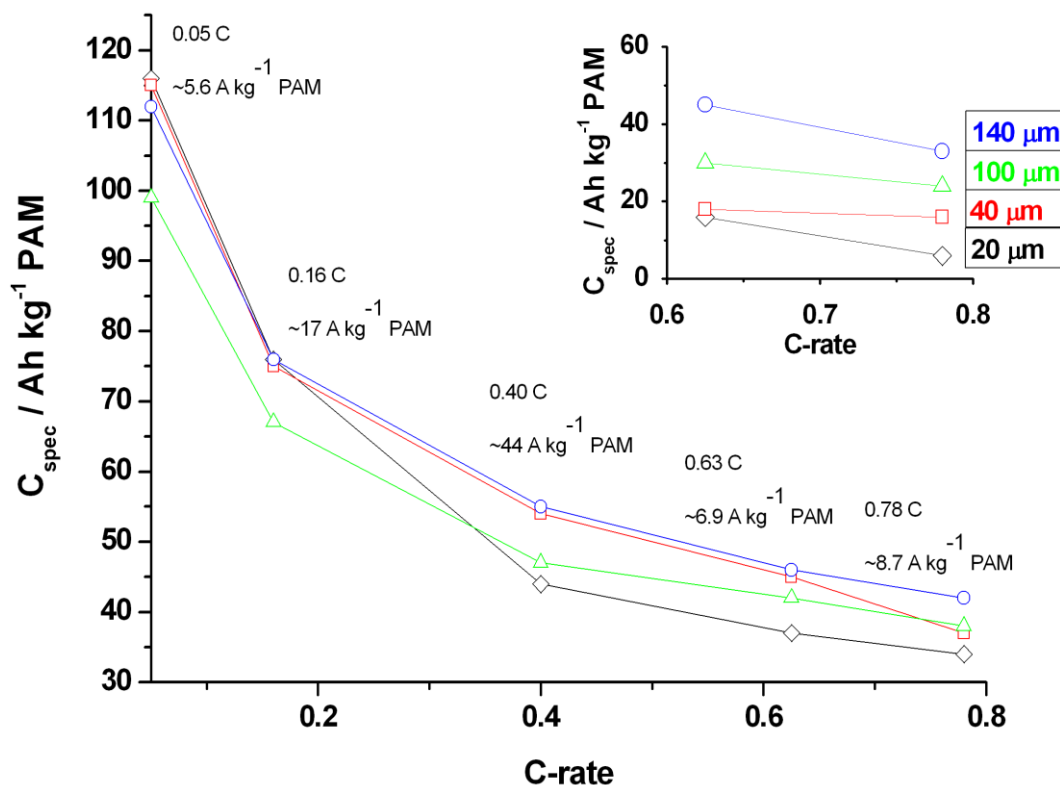
**Table 1.** Design parameters of the complete, cured lead-acid battery positive plates with lead layers of different thickness.

2Ah positive plate	Collector mass, $C_m \text{ g}^{-1}$	Plate mass, $P_m \text{ g}^{-1}$	Grid surface, $S \text{ cm}^{-2}$	N, $C_m P_m^{-1}$	PAM-to-grid surface ratio ( $\gamma$ ), $\text{g cm}^{-2}$	20-hour plate capacity, $\text{Ah kg}^{-1}$
RVC/Pb grid ( $d_{pb} = 20\mu\text{m}$ )	1,6	19,5	39	8%	0,5	107
RVC/Pb grid ( $d_{pb} = 40\mu\text{m}$ )	2,5	20,7	39	12%	0,5	101
RVC/Pb grid ( $d_{pb} = 100\mu\text{m}$ )	4,9	22,7	39	22%	0,5	78
RVC/Pb grid ( $d_{pb} = 140\mu\text{m}$ )	6,9	25,3	39	27%	0,5	83
Typical Pb-Ca VRLA grid	~13	~31	~28	42%	2,0-2,5	~66

Data presented in Table 1 [34] shows that the mass benefit for the positive plates based on RVC/Pb is relatively big even for lead coatings thicker than 100  $\mu\text{m}$ . For constant  $\gamma = 0.5$  [33], the N coefficient for the RVC-based plate will reach 40% - a value for a positive plate of standard construction, with ca. 300  $\mu\text{m}$  of lead coating.



**Figure 6.** Constant-current (0.78C) discharging profiles for RVC/Pb based plates with different thicknesses of lead layer covering RVC matrix.



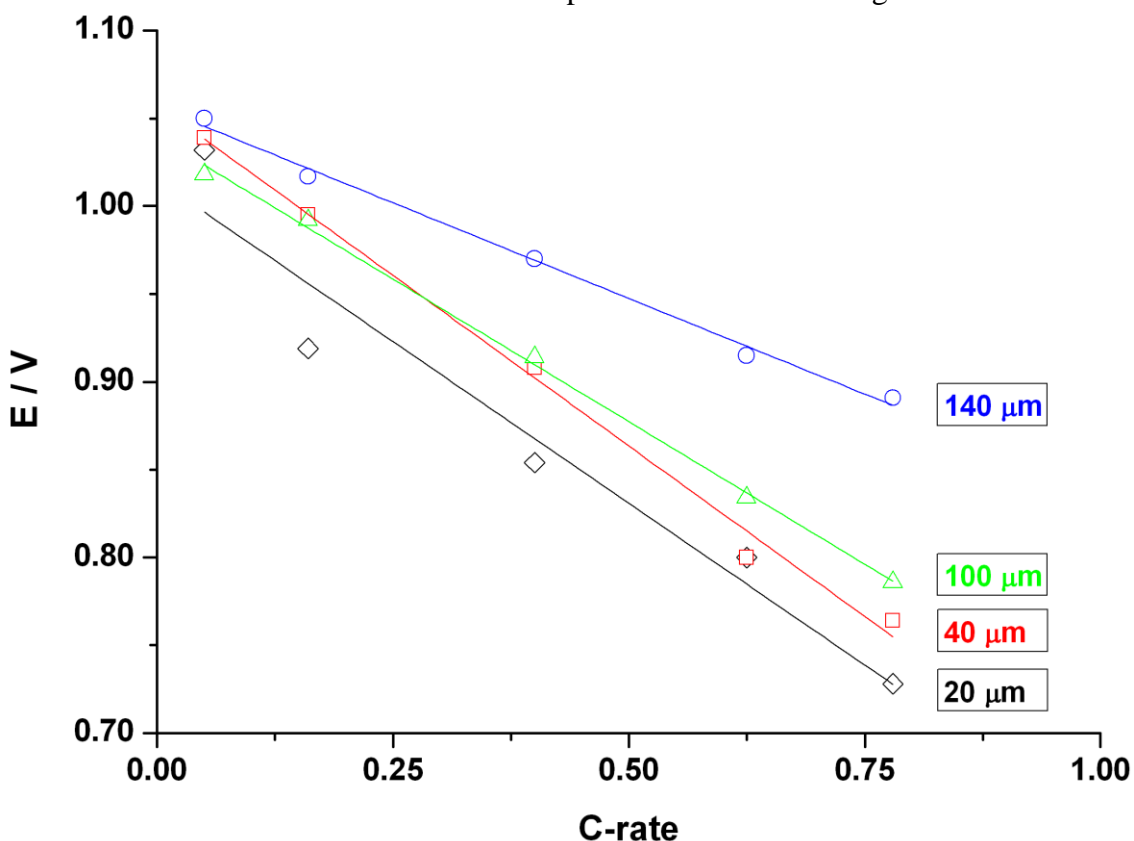
**Figure 7.** Dependence of specific capacity on discharging current for RVC/Pb based plates with different thicknesses of lead layer covering RVC matrix. Inset: discharging capacity for high currents and cutoff potential of 0.8 V.

Fig. 6 presents constant-current discharge curves for the RVC/Pb-based plates with layers of different thickness of Pb deposited on the RVC matrix [34]. For the RVC/Pb-based plates the discharge current was 0.78 C. Considering the discharge curves in Fig. 6 it is clear that the discharge voltage at elevated currents depends strongly on the thickness of the lead layer covering the RVC current collector. Fig. 7 presents the apparent specific capacity plotted against the discharge current for the positive plates with the RVC collectors covered with lead layers of different thickness [34]. At high loads, the apparent PAM capacity is considerably higher for plates having collectors with thicker layers of lead. This is seen even better for capacity data determined for a higher cutoff potential (inset to Fig. 7) and it might be explained in terms of a lower ohmic drop for the thicker lead layer covering the RVC matrix. As can be seen in Fig. 6, the plate with the 140-μm lead layer provided the highest discharging voltage, while the lowest discharging voltage was recorded for the plate with the 20-μm lead layer.

Although the 0.05 C discharge performance was not ordered according to the PAM amount or the lead layer thickness (see Fig. 7 and capacity data in Table 1) probably due to some bulk-PAM structural differences between the plates becoming important at deep discharging, the ohmic drop became the capacity-limiting factor during shallow discharging at high current. In Fig. 7 it is visible that the plate with the 100-μm lead layer had, relatively, the lowest capacity under the mild discharging regime (0.05 C, 0.16 C), but the discharging performance for 0.78 C was better than for the plates with thinner layers of lead (20 and 40 μm). The limiting by the ohmic drop is confirmed by the Peukert

dependence presented in the inset to Fig. 7 showing the positive plate apparent specific capacity reached at the relatively high positive plate cutoff potential (0.8 V vs.  $\text{Hg}/\text{Hg}_2\text{SO}_4$ ). It is also notable that the discharge time at 0.78 C is about 50% shorter than expected for a 5-Ah positive plate. This effect is probably due to several reasons. The reason, which has the greatest impact seems to be the low electronic conductivity of tetragonal  $\text{PbO}$ , the corrosion layer-forming compound. Tet- $\text{PbO}$  is formed in substantial amounts in the corrosion layer of non-alloyed lead grids during their anodizing in sulfuric acid [35]. A question also arises: does the considerable thickness of our plates (5-6 mm) influence the discharging performance at currents close to 1 C? The answer is related to the effective concentration of sulfuric acid in the micropores of the PAM. It is known that for elevated currents  $\text{PbSO}_4$  tends to precipitate on the plate surface, rather than in the plate interior [36].  $\text{PbSO}_4$  layer is impermeable to sulfate ions [37]. Consequently the relative amount of discharged PAM at the end of the discharge to the total amount of PAM in the plate will drop with increasing thickness of the plate. However, this effect seems to have a minor influence on limiting the discharge capacity at currents close to 1C.

The influence of the Pb coating thickness on the discharging performance of the RVC-based positive plates is clearly seen in the cell voltage versus the discharging current plots. Figs. 8 and 9 present the  $U=f(I)$  dependencies at two DODs, 25 % (Fig. 8) and 10 % (Fig. 9). One can see that the thinner the Pb coating, the higher the absolute value of the slope of the  $U=f(I)$  plot. Having in mind that the plates had the same PAM structures and the same treatment history, the only explanation for this behavior is the existence of different ohmic drops in the metallic coatings themselves.



**Figure 8.** Discharging voltage versus discharging current after drawing 0.5 Ah from cells having RVC/Pb based plates with different thicknesses of lead covering RVC matrix.

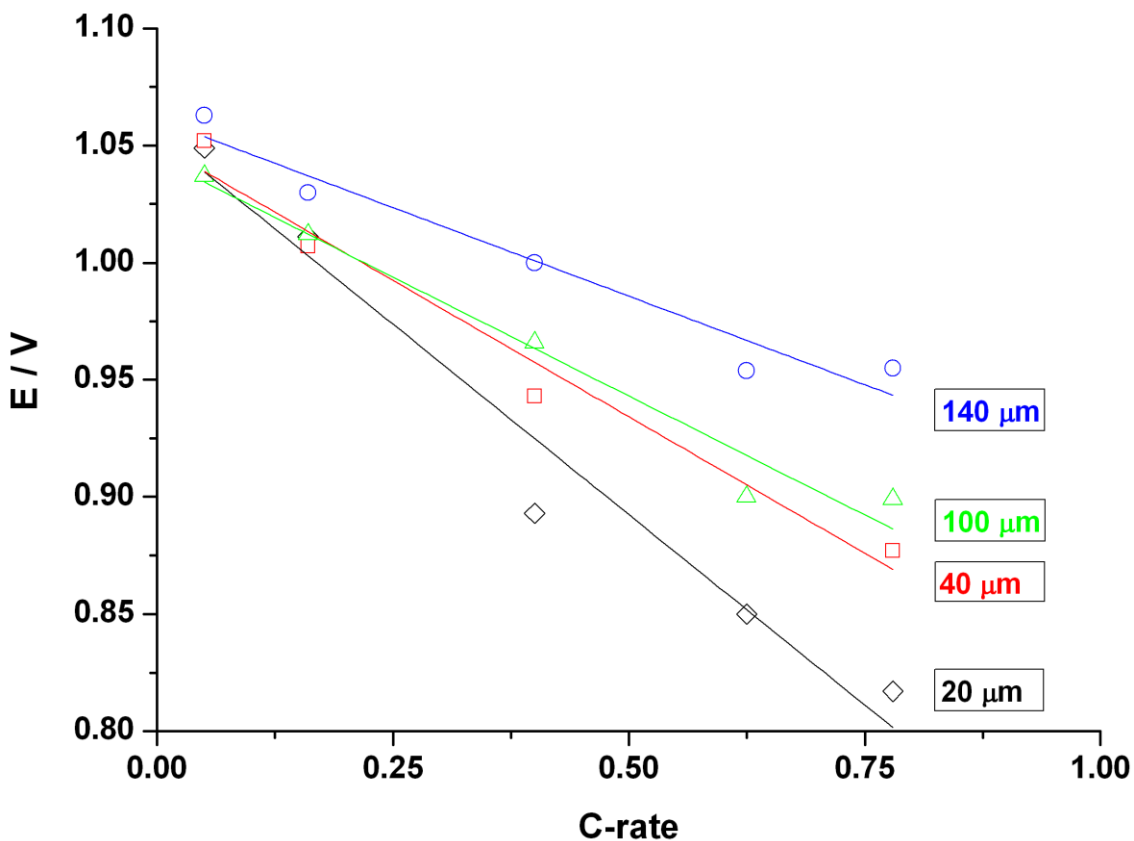


**Figure 9.** Discharging voltage versus discharging current after drawing 0.2 Ah from cells having RVC/Pb based plates with different thicknesses of lead covering RVC matrix.

After 18 charge/discharge cycles at 100% DOD the internal resistance of the cells has been measured. The internal resistance values for four cells with the RVC matrix covered with lead layers of 140 μm, 100 μm, 40 μm, and 20 μm were 25 mOhm, 25 mOhm, 130 mOhm, and 200 mOhm, respectively.

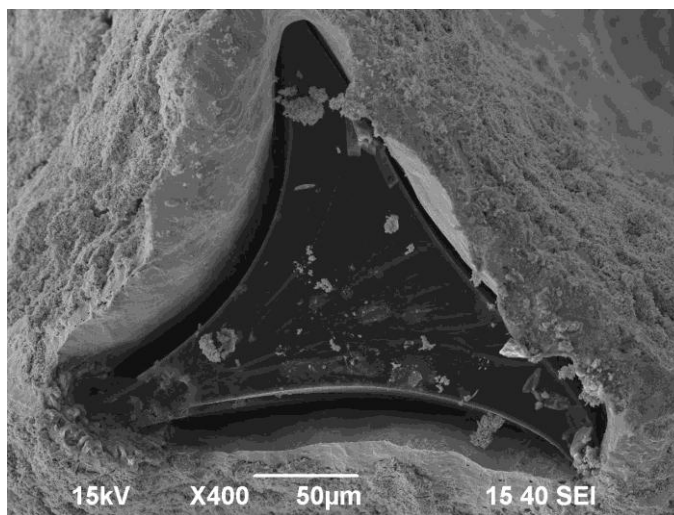


**Figure 10.** SEM image of positive-plate RVC/Pb current collector (lead coating thickness 60 μm) after 18 charging/discharging cycles at 100% DOD.

To compare the positive plate condition after operation, the cells were disassembled, the positive plates washed with water, cut horizontally, and sonicated in ammonium acetate to clean the cross section from Pb(II) species. Figs. 10 present the cross sections of the RVC/Pb grids taken from the positive plates with Pb layer thicknesses of 60 microns. The grid with the thinner Pb layer started to deteriorate after smaller amount of cycles. The lead layer became corroded. The RVC matrix lost its shape and color and deep cracks inside the RVC matrix were found. On the other hand, the grid with the thicker layer of lead preserved good mechanical properties. After sonicating in ammonium acetate, a shiny lead layer could be clearly visible without magnification and the plate kept its rigidity. The RVC matrix below the Pb layer remained unaltered.

A cyclic lifetime plot for the new type plates is presented in Fig. 11. The plates were discharged fully at 0.05 C (end of discharging at 1,75 V cell voltage). It is clearly seen that the thin RVC-supported 20 micron lead layer failed after a dozen cycles, while the 60- $\mu\text{m}$  lead layer sustained over 40 cycles at 100% DOD. The failure of the 60- $\mu\text{m}$  lead layer was uncertain as the cause of the end of life because both the active mass and the current collector were visibly deteriorated. The worn plate collector was much softer than the fresh one, so the plate could be broken quite easily. Also, the active mass had a very soft consistency and was shedding heavily off the plate. It has to be noted that much longer service life should not be expected from pure lead grid-based positive plates working in an excess of acid and at the given charging/discharging conditions.

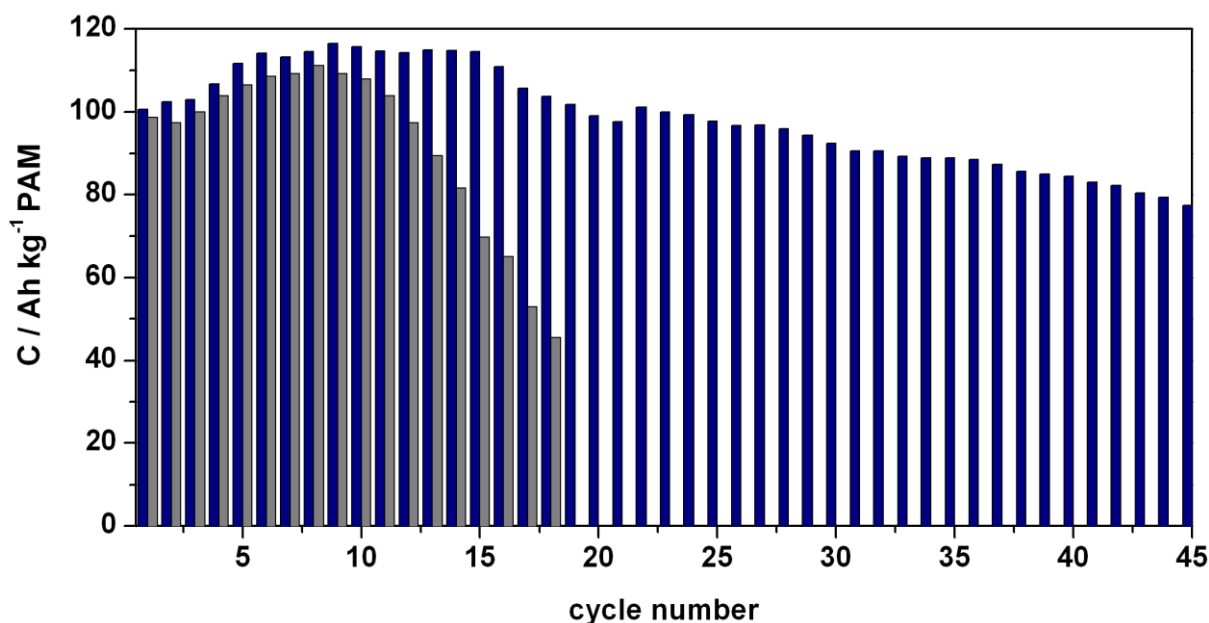


**Figure 11.** Cyclic capacity for RVC/Pb based positive plates with lead layers of different thickness covering RVC matrix (blue - 60 microns, gray – 20 microns). 100% DOD, discharging current 0.05 C.

Fig. 12 presents one charge/discharge cycle for a complete, 2-V lead-acid battery having one positive plate with lead-plated (60  $\mu\text{m}$ ) RVC grid and one negative plate with the grid made of RVC

plated with 20  $\mu\text{m}$  of lead. The nominal capacity of the cell was 2 Ah. The cell was working in an excessive amount of 35%  $\text{H}_2\text{SO}_4$ .

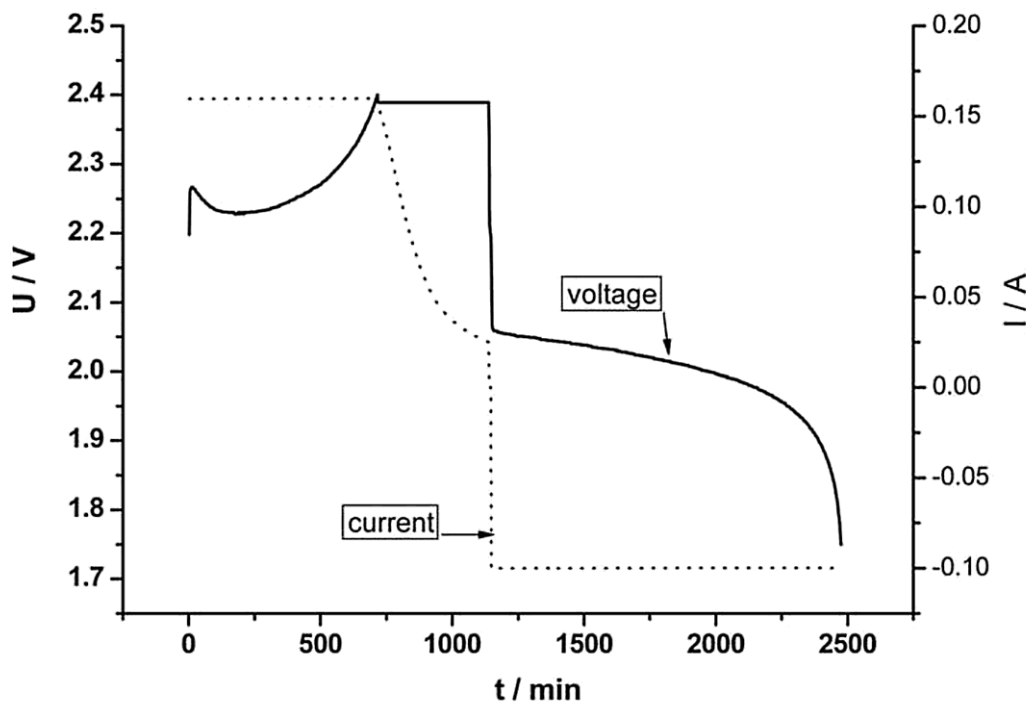


**Figure 12.** Charging/discharging characteristic of complete 2-V, 2-Ah lead-acid cell with plates based on RVC.

The specific energy of the new battery with the RVC/Pb-based plates at the discharging current of 0.05 C can be estimated at about 50 Wh/kg, which is ca. 50% higher than standard lead grid batteries and matches the specific energy for the Ni-Cd system [38].

#### 4. CONCLUSIONS

The results of this work show that the perspective of designing lead-acid batteries with significantly reduced weight is possible. Experiments showed that positive plates employing lightweight RVC/Pb grids can be prepared employing industrial methods and work successfully in the lead-acid batteries. The positive active mass efficiency was at the level of 120 Ah/kg, which is the PAM capacity of standard positive and much better than was expected for the thick plate design. Obviously, the specific plate capacity was higher for thinner Pb coatings, however, the optimal lead layer thickness was a tradeoff between the charging/discharging performance and the plate mass benefit. For the Pb coatings on the RVC as thin as 20  $\mu\text{m}$  the plates showed an excellent collector-to-plate mass ratio (8%) and good 0.05 C discharging parameters but the cyclic lifetime was limited. The best results, both in terms of the cyclic life and the discharging performance, were obtained for plates employing the RVC/Pb collector with the Pb layer thicker than 100  $\mu\text{m}$ , for which the collector-to-plate mass ratio, N, was about 22%, in comparison to 40% for standard plates. Improving the high

power performance and cycle life while keeping this mass benefit requires optimization of the coating composition using corrosion reducing additives. The specific energy of the new lead acid battery with the positive and the negative plates based on the RVC matrix/collector can reach the level of the Ni-Cd system.

#### ACKNOWLEDGEMENTS

This work was supported by National Center for Research and Development through grant INNOTECH-K1/IN1/47/152819/NCBR/12. The authors also gratefully acknowledge the help of the JENOX Akumulatory (Chodzież, Poland) in the preparation of battery plates.

#### References

1. A. Czerwiński, Patent RP, No. 167796 (1992)
2. M. Żelazowska, A. Czerwiński, *LABAT Extended Abstracts*, Varna, 1996, 107
3. A. Czerwiński, M. Żelazowska, Patent RP, No. 178258 (1995)
4. A. Czerwiński, M. Żelazowska, Patent RP, No. 180939 (1995)
5. A. Czerwiński, M. Żelazowska, *J. Electroanal. Chem.*, 410 (1996) 53
6. A. Czerwiński, M. Żelazowska, *J. Power Sources*, 64 (1997) 29
7. I. Paleska, R. Pruszkowska-Drachal, J. Kotowski, Z. Rogulski, J. D. Milewski, A. Czerwiński, *J. Power Sources*, 129 (2004) 326
8. A. Czerwiński, Z. Rogulski, H. Siwek, S. Obrębowski, I. Paleska, M. Chotkowski, M. Łukaszewski, *J. Appl. Electrochem.*, 39 (2009) 559
9. Z. Rogulski, W. Lewdorowicz, W. Tokarz, A. Czerwiński, *Pol. J. Chem.*, 78 (2004) 1357
10. A. Czerwiński, M. Dmochowska, M. Grden, M. Kopczyk, G. Wójcik, G. Młynarek, J. Kołata, J.M. Skowroński, *J. Power Sources*, 77 (1999) 28
11. Z. Rogulski, A. Czerwiński, *J. Power Sources*, 114 (2003) 176
12. M. Łukaszewski, A. Żurowski, A. Czerwiński, *J. Power Sources*, 185 (2008) 1598
13. Z. Rogulski, A. Czerwiński, *J. Solid State Electrochem.*, 7 (2003) 118
14. J. Wróbel, K. Wróbel, J. Lach, J. Dłubak, P. Podsadni, Z. Rogulski, I. Paleska, A. Czerwiński, *Przem. Chem.*, 93/3 (2014) 331
15. Firefly International Energy Co., <http://www.fireflyenergy.com>
16. A. Czerwiński, S. Obrębowski, J. Kotowski, Z. Rogulski, J.M. Skowroński, M. Bajsert, M. Przysiałowski, M. Buczkowska-Biniecka, E. Jankowska, M. Baraniak, J. Rotnicki, M. Kopczyk, *J. Power Sources*, 195 (2010) 7524
17. A. Czerwiński, S. Obrębowski, J. Kotowski, Z. Rogulski, J. Skowroński, M. Bajsert, M. Przysiałowski, M. Buczkowska-Biniecka, E. Jankowska, M. Baraniak, J. Rotnicki, M. Kopczyk, *J. Power Sources*, 195 (2010) 7530
18. A. Czerwiński, S. Obrębowski, J. Kotowski, M. Bajsert, M. Przysiałowski, Patent RP, No. 211599 (2009)
19. A. Czerwiński, S. Obrębowski, J. Kotowski, M. Bajsert, M. Przysiałowski, Patent RP, No. 211918 (2009)
20. Y. Jang, N.J. Dudney, T.N. Tiegs, J. W. Klett, *J. Power Sources*, 161 (2006) 1392
21. Y. Chen, B.Z. Chen, X.C. Shi, H. Xu, W. Shang, Y. Yuan, L.P. Xiao, *Electrochim. Acta*, 53 (2008) 2245
22. Y. Chen, B.Z. Chen, L.W. Ma, Y. Yuan, *Electrochem. Commun.*, 10 (2008) 1064
23. Y. Chen, B.-Z. Chen, L.W. Ma, Y. Yuan, *J. Appl. Electrochem.*, 38 (2008) 1409
24. A. Dekanski, *Carbon*, 39 (2001) 1195

25. K. Das, A. Mondal, *J. Power Sources*, 35 (1995) 251
26. K. Das, A. Mondal, *J. Power Sources*, 89 (2000) 112
27. E. Gyenge, J. Jung, B. Mahato, *J. Power Sources*, 113 (2003) 388
28. E. Gyenge, J. Jung, Patent No. WO03028130
29. L.W. Ma, B.Z. Chen, Y. Chen, Y. Yuan, *J. Appl. Electrochem.*, 39 (2009) 1609
30. A. Kirchev, N. Kircheva, M. Perrin, *J. Powers Sources*, 196 (2011) 8773
31. A. Czerwiński, S. Obrębowski, Z. Rogulski, *J. Power Sources*, 198 (2012) 378
32. ERG Materials and Aerospace Corporation, Duocel® Carbon Foam Surface Area, <http://www.ergaerospace.com/surface-area.html>
33. D. Pavlov, *J. Power Sources*, 53 (1995) 9
34. A. Czerwiński, S. Obrębowski, Z. Rogulski, J. Kotowski, *LABAT Extended Abstracts*, Albena, 2011, 37
35. D. Pavlov, *J. Electrochem. Soc.*, 117 (1970) 1103
36. Z. Ziętkiewicz, *Akumulatory*, WKŁ, Warszawa, 1983
37. P. Ruetschi, *J. Electrochem. Soc.*, 120 (1973) 331
38. D. Linden, T.B. Reddy, *Handbook of Batteries*, McGraw-Hill, New York, 1993

© 2014 The Authors. Published by ESG ([www.electrochemsci.org](http://www.electrochemsci.org)). This article is an open access article distributed under the terms and conditions of the Creative Commons Attribution license (<http://creativecommons.org/licenses/by/4.0/>).